

Strength regularity and failure criterion of plain HSHPC under biaxial compression after exposure to high temperatures

He Zhenjun Song Yupu

(State Key Laboratory of Coastal and Offshore Engineering, Dalian University of Technology, Dalian 116024, China)

Abstract: Biaxial compression tests are performed on 100 mm × 100 mm × 100 mm cubic specimens of plain high-strength high-performance concrete (HSHPC) at seven kinds of stress ratios, $\sigma_2 : \sigma_3 = 0 : -1, -0.20 : -1, -0.30 : -1, -0.40 : -1, -0.50 : -1, -0.75 : -1$, and $-1.00 : -1$ after exposure to normal and high temperatures of 20, 200, 300, 400, 500 and 600 °C, using a large static-dynamic true triaxial machine. Friction-reducing pads are three layers of plastic membranes with glycerine in-between for the compressive loading plane. Failure modes of the specimens are described. The two principally static compressive strengths are measured. The influences of the temperatures and stress ratios on the biaxial strengths of HSHPC after exposure to high temperatures are also analyzed. The experimental results show that the uniaxial compressive strength of plain HSHPC after exposure to high temperatures does not decrease completely with the increase in temperature; the ratios of the biaxial to its uniaxial compressive strengths depend on the stress ratios and brittleness-stiffness of HSHPC after exposure to different high temperatures. The formula of the Kupfer-Gerstle failure criterion modified with the temperature and stress ratio parameters for plain HSHPC is proposed.

Key words: high-strength high-performance concrete (HSHPC); high temperatures; stress ratio; uniaxial and biaxial compressive strength; failure criterion

Concrete has been the leading construction material for nearly a century. In recent years, high performance concrete (HPC) is becoming an attractive alternative to traditional normal strength concrete (NSC). The alleged HPC is generally defined as high-strength, high fluidity, high durability concrete or to possess one of these characteristics; moreover, high-performance water reducer and superfine mineral admixtures are absolutely necessary ingredients. The dense microstructure of high-strength concrete (HSC) ensures high strength and very low permeability, so that it has a relatively low weak deformation capability or much higher “brittleness-stiffness” when compared to NSC. Recent fire test results show that there is a great difference between the properties of HSC and NSC after exposure to high temperatures^[1]. It is observed that HSC is susceptible to spalling, or even explosive spalling when subjected to rapid temperature rises as in the case of a fire^[2]. Hence, one of the main concerns for the usage of HSHPC in fire resistance applications is its performance under fire conditions. It is well known that

conventional analysis and design methods of reinforced concrete are generally still based upon material properties obtained from the basic uniaxial strength test, although we know that a true uniaxial condition in structures is extremely rare. In practice, many concrete structures such as spiral columns and their mode of building and nuclear reactor pressure containers are under multiaxial stress states. At the same time, with the wide use of computers, the finite element method and HSHPC in concrete structures, it has become increasingly evident that it is quite important and urgent for experimental studies on the mechanical properties of HSHPC under multiaxial stress states, and for studies on the design and analysis of nonlinear behavior designs of reinforced concrete structures based upon multiaxial mechanical behavior. So, many researchers have paid much attention to HSHPC at home and abroad. Late in the 1960s, some researchers^[3] began to perform experimental studies of NSC under multiaxial stress states in order to design nuclear reactor containers and so on. But, until now, most studies^[4] have been carried out to characterize the mechanical behavior of HSC or HPC under uniaxial stress states, or NSC under multiaxial stress states. However, literature on the mechanical behavior of HSC or HPC under multiaxial loadings is extremely scarce; moreover, among them, most of the tests of confined compression (with two equal stresses) behavior of concrete has been performed under triaxial stress states using cylindrical specimens subjected to hydrostatic pressure in a triaxial cell and axial loading. Lu and Thomas^[5] studied the mechanical behavior of HSC and steel fiber reinforced high strength concrete under uniaxial and triaxial compression, when testing $\phi 100 \text{ mm} \times 200 \text{ mm}$ and $\phi 100 \text{ mm} \times 150 \text{ mm}$ cylinder specimens lubricated with a combination of two 0.125 mm thick teflon sheets on the top of one layer of 0.015 mm thick aluminum foil. The previous investigations conducted on the effects of high temperature on properties of plain HSC or HPC have also merely focused on the behavior of strength and deformation under uniaxial loading. However, literature on the mechanical properties of plain HSC or HPC under multiaxial stress states under high temperatures, has not been documented. Luo et al.^[6] stated that the strength of HPC degenerates more severely and has a higher residual strength than that of NSC after exposure to high temperatures. Chan et al.^[7] stated that the range between 400 °C and 800 °C is critical to the strength loss of concrete causing a large percentage of loss of strength. This paper presents the strength regularities and failure criteria of HSHPC with seven kinds of different stress ratios under biaxial compressive loading after exposure to six temperature levels, using a large static-dynamic true triaxial machine. The biaxial compression tests are performed on 100 mm × 100 mm × 100 mm cubic concrete specimens. This paper may al-

Received 2007-08-14.

Biographies: He Zhenjun (1975—), male, graduate; Song Yupu (corresponding author), male, doctor, professor, syupu@dlut.edu.cn.

Citation: He Zhenjun, Song Yupu. Strength regularity and failure criterion of plain HSHPC under biaxial compression after exposure to high temperatures[J]. Journal of Southeast University (English Edition), 2008, 24(2): 206 – 211.

so serve as a reference (testing data, correlated formula and mechanical behavior) for the maintenance, design and the life prediction of HSHPC structure subjected to high temperatures, for example, fire, etc.

1 Materials and Experimental Procedures

1.1 Materials and mix proportion

The cementitious materials used for this investigation are Chinese standard P · I 52.5R Portland cement (standard compressive strength of higher than 52.5 MPa at the age of

28 d) and one-level fly ash^[8]. The coarse aggregate is crushed stone (diameters ranging from 5 to 20 mm) and the fine aggregate is natural river sand (fineness modulus of 2.7); water is tap-water. Tab. 1 shows the mix proportions by weight of the mixture and the major parameters of the HSHPC (f_c is the uniaxial compressive strength of 100 mm × 100 mm × 100 mm cubic HSHPC specimens with friction-reducing pads prior to high temperatures, and its strength value is about equal to that of 150 mm × 150 mm × 300 mm prisms.).

Tab. 1 Mix proportion and major parameters of the HSHPC

Strength level	Water-cementitious ratio	Water/ ($\text{kg} \cdot \text{m}^{-3}$)	Cement/ ($\text{kg} \cdot \text{m}^{-3}$)	Fly ash/ ($\text{kg} \cdot \text{m}^{-3}$)	Fine aggregate/ ($\text{kg} \cdot \text{m}^{-3}$)	Coarse aggregate/ ($\text{kg} \cdot \text{m}^{-3}$)	Super-plasticizer/ ($\text{kg} \cdot \text{m}^{-3}$)	Slump/ cm	Compressive strength f_c /MPa
HSHPC	0.31	175	470	94.52	615.77	1 094.71	6.77	24	60.16

1.2 Samples and testing methods

1.2.1 Casting and curing of specimens

The coarse aggregate and the fine aggregate are mixed for about 1 min when a portion of the proportional water was being sprayed on them, and then the cement and one-level fly ash are added in turn; after that, the residual proportional water with SiKa^(R) NF-III superplasticizer (There are also the properties of increasing slump, durability and retardation besides the performance of ordinary water reducing agents.) is added slowly over a period of 1 min. Finally these ingredients are mixed for 2 to 3 min^[8]. All the specimens cast in steel molds and compacted slightly by vibrating table are demoulded after 24 h of the casting and then cured under conditions of $(20 \pm 3)^\circ\text{C}$ and 95% RH (relative humidity) for 28 d according to GB J82—85 (The test method of long-term and durability on ordinary concrete), and they are then stored at a natural temperature outside. The age of the specimens tested is about one year.

The concrete specimens tested are in 100 mm × 100 mm × 100 mm, 150 mm × 150 mm × 150 mm or 150 mm × 150 mm × 300 mm. The 100 mm concrete cubes are used to measure the strength for biaxial compression test. For determination of the strength grade for the HSHPC and the strength of the prism, each batch is cast in six 150 mm cubic specimens, and six 150 mm × 150 mm × 300 mm prismatic specimens.

1.2.2 Apparatus and testing methods

The tests of high temperatures and biaxial compression are performed in the State Key Laboratory of Coastal and Off-shore Engineering of Dalian University of Technology.

The specimens in the high temperatures tests are 100 mm cubes. For each stress ratio, at least six specimens are heated up. These 100 mm cubic specimens are elevated to peak tem-

peratures of 200, 300, 400, 500 and 600 °C at a heating rate of 10 °C/min, respectively. After the peak temperature is reached, it is maintained for 6 h; the time of furnace cooling is about 1 h; then, the specimens are cooled naturally to room temperature. These specimens are performed in a multi-axial testing machine after 24 h. In this study, the surfaces of all the specimens are dry before being exposed to high temperatures. No explosive spalling is observed during the fire test on the HSHPC specimens with temperatures ranging from 200 to 600 °C.

The mechanical tests are conducted in a triaxial testing machine that is capable of developing three independent compressive or tensile forces. The biaxial compression process is necessary to insure uniform dimensions for each cubic specimen. The major stress direction is always applied perpendicularly to the surface of the specimens. The proportional loading modes ($\sigma_2 : \sigma_3$) are employed. All the specimens are tested at a loading speed of 0.3 to 0.5 MPa/s in the direction of σ_3 , with friction-reducing pads (three layers of butter and three layers of plastic membrane) placed between the platens and the specimens for all tests. Seven stress ratios $\sigma_2 : \sigma_3 = 0 : -1, -0.20 : -1, -0.30 : -1, -0.40 : -1, -0.50 : -1, -0.75 : -1, -1.00 : -1$ under biaxial compressive loading after exposure to normal and high temperatures of 20, 200, 300, 400, 500, and 600 °C are tested. The principal stresses are expressed as $\sigma_1 \geq \sigma_2 \geq \sigma_3$ (compression denoted as negative and tension denoted as positive); three specimens are at least tested for each stress ratio and the test values are averaged after the discrete values are deleted. Fig. 1 shows the loading direction and the state of the specimen under uniaxial and biaxial compressions in the triaxial experimental machine, respectively.

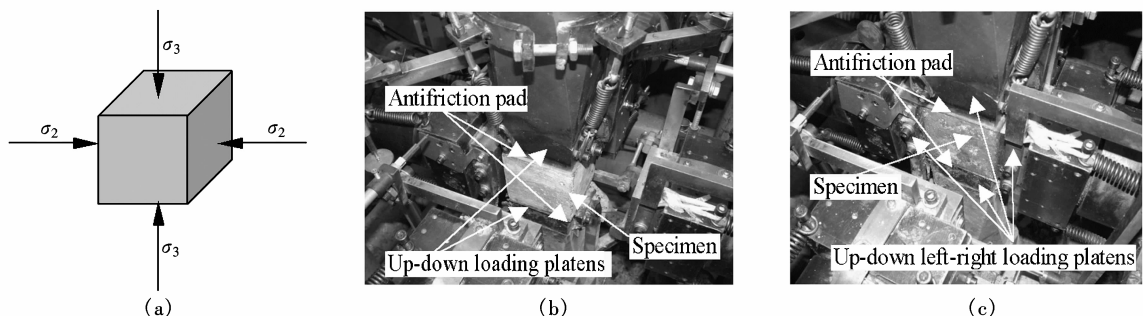


Fig. 1 Shape of the specimen in triaxial testing machine. (a) Loading direction; (b) Uniaxial compression; (c) Biaxial compression

2 Test Results and Discussion

2.1 Experimental results

The experimental results of plain HSHPC under biaxial compression after high temperatures are given in Tab. 2.

2.2 Failure modes

The surface deterioration and the failure modes of the HSHPC specimens under uniaxial and biaxial compression subjected to the action of high temperatures are shown in Fig. 2.

From Fig. 2, it is obvious that the influence of high temperature on HSHPC does not change the tensile splitting

mode from occurring. In Figs. 2 (a) and (b), the HSHPC specimen is split into multiple minor prisms (prism-type failure modes). As shown in Figs. 2 (c) and (d), there are parallel plate-type fragments on the surface of σ_2 and σ_3 under biaxial compressive loading; moreover, the number of cracks becomes greater as the stress ratio increases. The two failure modes mentioned above demonstrate that providing confinement stress along σ_2 directions will change the failure modes. Although the failure modes under uniaxial and biaxial loading are different, the failure cause is that the splitting tensile strain along the unloading planes is greater than the ultimate tensile strain of HSHPC.

Tab. 2 Biaxial compressive strength index of plain HSHPC under various stress ratios after high temperatures

Temperature levels/°C	Stress ratio $\sigma_2 : \sigma_3$	σ_{2f} /MPa	σ_{3f} /MPa	Temperature levels/°C	Stress ratio $\sigma_2 : \sigma_3$	σ_{2f} /MPa	σ_{3f} /MPa
20	0.00 : -1	0.00	-60.16	400	0.00 : -1	0.00	-49.70
	-0.20 : -1	-13.52	-67.58		-0.20 : -1	-11.41	-57.04
	-0.30 : -1	-20.99	-69.97		-0.30 : -1	-17.81	-59.36
	-0.40 : -1	-30.33	-75.83		-0.40 : -1	-24.67	-61.68
	-0.50 : -1	-36.93	-73.85		-0.50 : -1	-32.21	-64.41
	-0.75 : -1	-51.28	-68.37		-0.75 : -1	-45.21	-60.28
	-1.00 : -1	-66.78	-66.78		-1.00 : -1	-55.88	-55.88
200	0.00 : -1	0.00	-63.96	500	0.00 : -1	0.00	-35.72
	-0.20 : -1	-14.42	-72.10		-0.20 : -1	-8.38	-41.91
	-0.30 : -1	-20.69	-68.98		-0.30 : -1	-13.72	-45.73
	-0.40 : -1	-29.06	-72.65		-0.40 : -1	-18.70	-46.74
	-0.50 : -1	-36.80	-73.59		-0.50 : -1	-25.36	-50.72
	-0.75 : -1	-53.22	-70.96		-0.75 : -1	-35.78	-47.70
	-1.00 : -1	-67.48	-67.48		-1.00 : -1	-42.26	-42.26
300	0.00 : -1	0.00	-61.64	600	0.00 : -1	0.00	-24.90
	-0.20 : -1	-13.03	-65.16		-0.20 : -1	-5.98	-29.90
	-0.30 : -1	-21.21	-70.70		-0.30 : -1	-10.15	-33.83
	-0.40 : -1	-28.54	-71.35		-0.40 : -1	-14.18	-35.46
	-0.50 : -1	-37.59	-75.18		-0.50 : -1	-18.31	-36.61
	-0.75 : -1	-53.08	-70.77		-0.75 : -1	-25.39	-33.85
	-1.00 : -1	-66.69	-66.69		-1.00 : -1	-30.65	-30.65

Note: σ_{2f} and σ_{3f} are the biaxial compressive strengths, respectively.

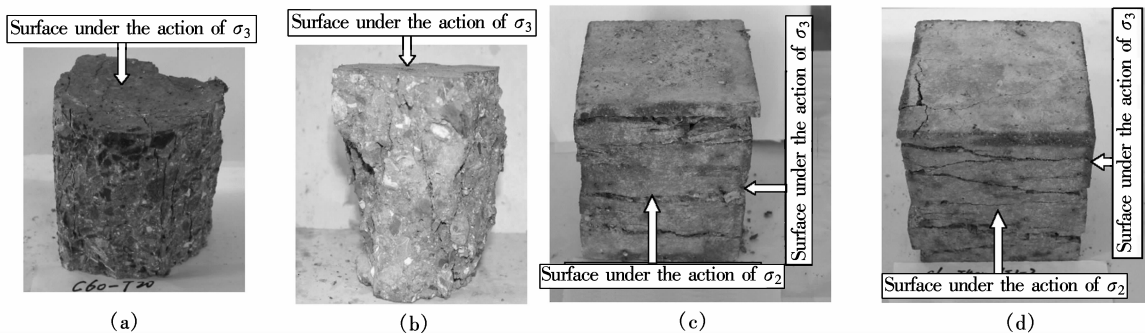


Fig. 2 Failure modes of plain HSHPC under uniaxial and biaxial compressions at different temperature levels. (a) Prism-type failure after 20 °C; (b) Prism-type failure after 600 °C; (c) Plate-type failure after 200 °C; (d) Plate-type failure after 400 °C

2.3 Strength characteristics

Fig. 3(a) shows the influence regularity of the stress ratio on the principal strength σ_{3f} at different temperature levels. It can be seen that the biaxial σ_{3f} is greater than the corresponding uniaxial compressive strength at the same temperature levels for all stress ratios. In addition, the biaxial stress ratio corresponding to the maximum σ_{3f} is 0.40 or 0.50.

The change of σ_{3f} is dependent on the biaxial stress ratio at the same temperature levels. The influence of the stress ratio on σ_{3f} changes approximately by the parabolic-like curve at every temperature level. The uniaxial compressive strength at high temperatures decreases gradually around 400 °C with the increase in temperature. So, the temperatures around 400 °C are critical to the ultimate strength. (Note: The trend curves of Figs. 3(a) and (b) at 20 °C and 300 °C are nearly

coincidental.)

Figs. 3(b) and (c) give the relationships between stress ratios and the ratios of the biaxial to uniaxial compressive strengths prior to and after high temperatures at different temperature levels, respectively. From Fig. 3(b), it is apparent that after 200 °C and 300 °C, the values of $-\sigma_{3f}/f_c$ are greater than 1 for all stress ratios, which differs from the conclusions of the same research group on the NSC^[19]. It can be seen from Fig. 3(c), the times of $-\sigma_{3f}/f_c^T$ (f_c^T is the uniaxial compression strength with friction-reducing pads after different temperature levels.) is greater than 1 at all stress ratios for all temperature levels. In addition, the influence extent of the stress ratios on σ_{3f} is different at different temperature levels. For example, when σ_2/σ_3 is equal to 0.40 or 0.50, the strengths under biaxial compression is greater at

every temperature level; the values of $-\sigma_{3f}$ (−75.83, −73.59, −75.18, −64.41, −50.72, −36.61 MPa) after being exposed to normal and high temperature of 20, 200, 300, 400, 500, and 600 °C are 1.26, 1.22, 1.25, 1.07, 0.84, 0.61 times the uniaxial compressive strength (60.16 MPa) prior to high temperatures, respectively; but, they are 1.26, 1.15, 1.22, 1.30, 1.42, 1.47 times it (60.16, 63.96, 61.64, 49.7, 35.72, 24.9 MPa) at the corresponding temperature levels, respectively.

Fig. 3(d) demonstrates the influence regularity of the temperature levels on the principal strength σ_{3f} . It can be seen from Fig. 3(d) and Tab. 2 that σ_{3f} of the plain HSHPC does not decrease completely with the increase in temperature under the uniaxial and biaxial compression. After exposure to up to 200 °C and 300 °C, their uniaxial compressive

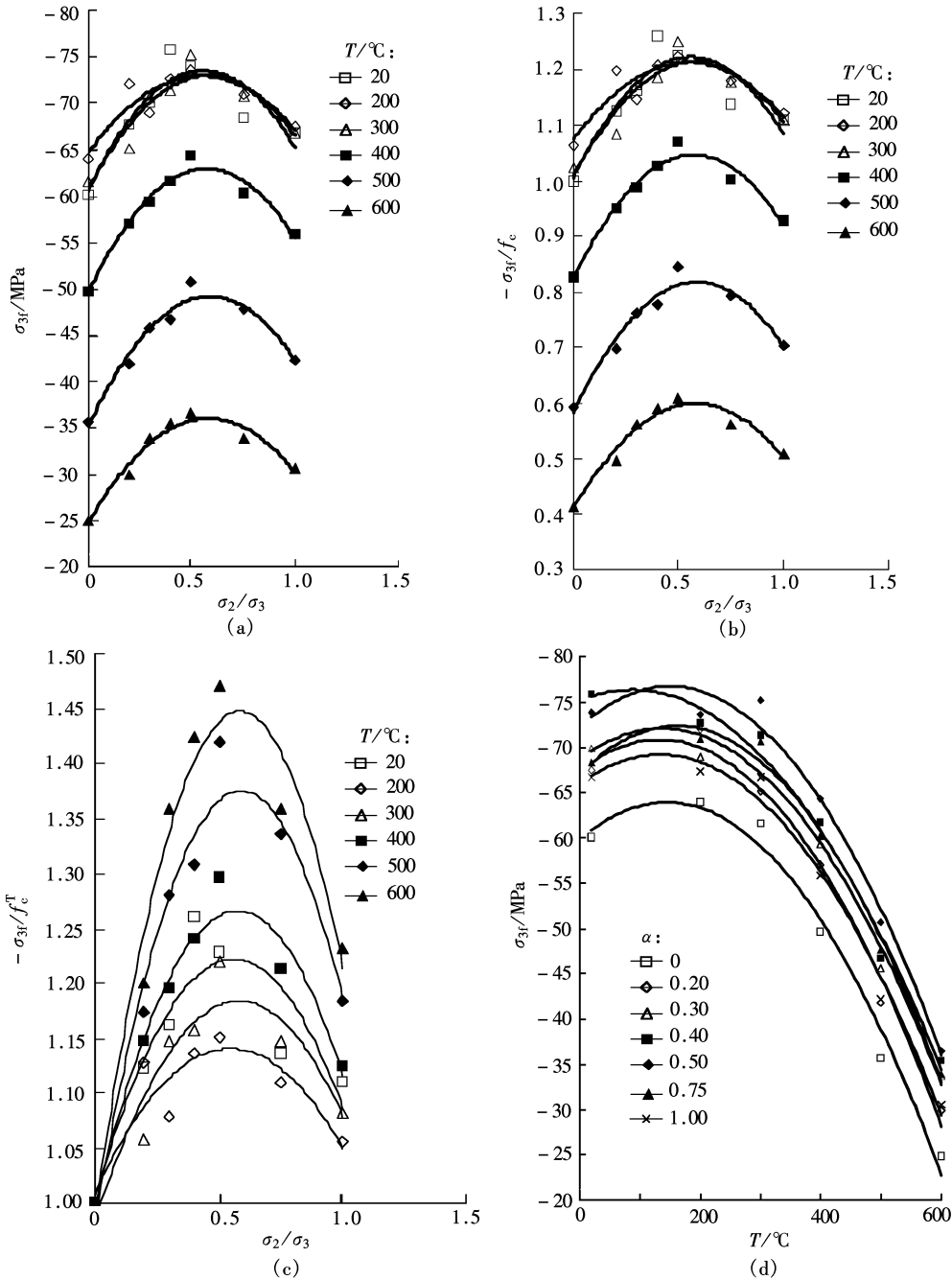


Fig. 3 Influence regularity of stress ratios and temperature levels on HSHPC strengths. (a) Influence of σ_2/σ_3 on σ_{3f} ; (b) Influence of σ_2/σ_3 on $-\sigma_{3f}/f_c$; (c) Influence of σ_2/σ_3 on $-\sigma_{3f}/f_c^T$; (d) Influence of temperatures on σ_{3f}

strengths are increased; but, after 200 °C, biaxial compression strengths under different stress ratios are partially increased; both the changes occur according to the parabolic-like curves with the increase in temperature.

Through the above discussion, it is indicated that the uniaxial compressive strength after exposure of up to 200 °C and 300 °C, is increased, and that their brittleness-stiffness is great; but, their times of $-\sigma_{3f}/f_c^x$ is decreased. So, the increasing times under biaxial compression depends on the brittleness-stiffness of the concrete after exposure to different temperature levels as well as the stress ratios. The greater the brittleness-stiffness of concrete after exposure to high temperatures is, the less the increasing time under biaxial compression.

Kupfer^[3] tested biaxial compressive concrete-strength of NSC at normal temperature, which is about 1.18 to 1.27 times uniaxial compressive strength when 200 mm × 200 mm × 50 mm plate specimens with brush-bearing platen as friction-reducing pads were used. The test results for Lee et al.^[10] indicated that the concrete strengths of NSC under biaxial compression ($\alpha = 1.00$ and $\alpha = 0.50$) at normal temperature are higher by about 17% and 28% on the average than those under the uniaxial compression. Comparing the test results at normal temperatures in this paper with those of Refs. [3, 10], there is not any significant difference in the ratios of the biaxial to uniaxial compressive strengths for HSHPC and NSC.

2.4 Failure criterion

The Kupfer-Gerstle formula with the temperature and stress ratio parameters under biaxial compression is obtained as follows:

$$\left(\frac{\sigma_{3f}}{f_c} + \frac{\sigma_{2f}}{f_c}\right)^2 + F_1(T)\frac{\sigma_{3f}}{f_c} + F_2(T)\frac{\sigma_{2f}}{f_c} = 0 \quad (1)$$

Eq. (1) is transferred to

$$\frac{\sigma_{3f}}{f_c} = \frac{F_1(T) + F_2(T)\alpha}{(1 + \alpha)^2} \quad (2)$$

where $\alpha = \sigma_2/\sigma_3$ ($0 \leq \alpha \leq 1$) is the stress ratio; T is the temperature level ($20 \leq T \leq 600$ °C); f_c is the uniaxial compressive strength of plain HSHPC prior to high temperatures; $F_1(T)$ and $F_2(T)$ are functions of T . Using regression analysis of test results (see Tab. 2) of plain HSHPC calculated by Eq. (2) at various temperature levels, the corresponding values of $F_1(T)$ and $F_2(T)$ are obtained, and then they are regressed with the corresponding temperature levels again. The formulae of $F_1(T)$ and $F_2(T)$ are as follows:

$$\left. \begin{aligned} F_1(T) &= 2.6425 \left(\frac{T}{1000}\right)^2 - 0.6571 \left(\frac{T}{1000}\right) - 0.9813 \\ R^2 &= 0.9906 \\ F_2(T) &= 9.5206 \left(\frac{T}{1000}\right)^2 - 2.8027 \left(\frac{T}{1000}\right) - 3.3708 \\ R^2 &= 0.9869 \end{aligned} \right\} \quad (3)$$

Fig. 4 gives the comparison of Eq. (2) and test values. It can be seen from Fig. 4 that the model of failure envelopes in principal stress space for HSHPC under biaxial compression

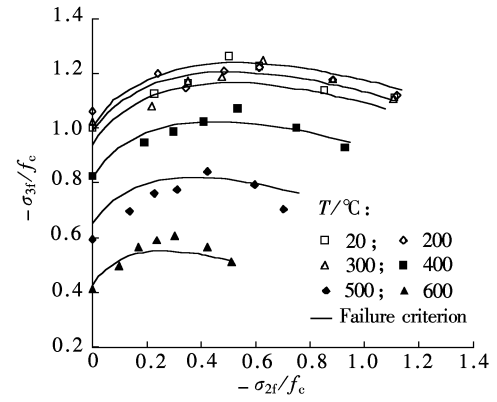


Fig. 4 The comparison of Eq. (2) and test values

after being subjected to high temperatures, is of better precision and applicability.

3 Conclusions

1) No explosive spalling is observed during the high temperature test on the 100 mm cubic specimens for HSHPC with temperatures ranging from 200 °C to 600 °C, if the specimens are dried prior to exposure to high temperatures.

2) The effect of high temperatures on plain HSHPC does not change the failure modes. The failure modes of HSHPC under uniaxial and biaxial compressions are prism-type and parallel plate-type shapes, respectively. The effects of confinement stresses can change the failure modes.

3) The ultimate strength σ_{3f} of HSHPC under biaxial compression for all stress ratios is greater than the corresponding uniaxial compressive strength at the same temperature level. The uniaxial compressive strength of plain HSHPC is not decreased after 200 and 300 °C. HSHPC specimens above 200 and 300 °C is higher in brittleness-stiffness than that above 400, 500, 600 °C. The temperature around 400 °C is critical to the ultimate strength that decreases rapidly. The increasing times of the biaxial to uniaxial compressive strength depends on the stress ratios, and the brittleness-stiffness of HSHPC above different temperature levels.

4) The formula of Kupfer-Gerstle failure criterion modified with the temperature and stress ratio parameters for plain HSHPC is proposed.

References

- [1] Li Min, Qian Chunxiang, Sun Wei. Mechanical properties of high-strength concrete after fire [J]. *Cement and Concrete Research*, 2004, **34**(6): 1001 – 1005.
- [2] Peng Gaifei, Yang Wenwu, Zhao Jie, et al. Explosive spalling and residual mechanical properties of fiber-toughened high-performance concrete subjected to high temperatures [J]. *Cement and Concrete Research*, 2006, **36**(4): 723 – 727.
- [3] Kupfer H. Behavior of concrete under biaxial stresses [J]. *ACI Journal*, 1969, **66**(8): 656 – 666.
- [4] Husem Metin, Gozutok Serhat. The effects of low temperature curing on the compressive strength of ordinary and high performance concrete [J]. *Construction and Building Materials*, 2005, **19**(1): 49 – 53.
- [5] Lu Xiaobin, Thomas Hsu Cheng-Tzu. Behavior of high strength concrete with and without steel fiber reinforcement in triaxial compression [J]. *Cement and Concrete Research*, 2006, **36**(9): 1679 – 1685.

[6] Luo X, Sun W, Chan Y N. Residual compressive strength and microstructure of high performance concrete after exposure to high temperature [J]. *Materials and Structures/Matériaux et Constructions*, 2000, **33**(6): 294 – 298.

[7] Chan Sammy Y N, Peng Gaifei, Chan John K W. Comparison between high strength concrete and normal strength concrete subjected to high temperature [J]. *Materials and Structures/Matériaux et Constructions*, 1996, **29**(12): 616 – 619.

[8] The High-strength High-performance Concrete Committee of the Chinese Civil Engineering Society. *Guide for structural*

design and construction of high-strength concrete [M]. Beijing: China Architecture and Building Press, 2001. (in Chinese)

[9] Qin Likun, Song Yupu, Zhang Zhong, et al. The research on strength and deformation of plain concrete under biaxial compression after high temperatures [J]. *Journal of Dalian University of Technology*, 2005, **45**(1): 113 – 117. (in Chinese)

[10] Lee Sangkeun, Song Youngchul, Han Sanghoon. Biaxial behavior of plain concrete of nuclear containment building [J]. *Nuclear Engineering and Design*, 2004, **227**(2): 143 – 153.

高温后高强高性能混凝土双轴压强度规律与破坏准则

何振军 宋玉普

(大连理工大学海岸与近海工程国家重点实验室, 大连 116024)

摘要: 利用大型静动真三轴试验机, 进行了常温 20 ℃ 以及 200, 300, 400, 500 和 600 ℃ 高温后高强高性能混凝土在 7 种应力比, $\sigma_2 : \sigma_3 = 0 : -1, -0.20 : -1, -0.30 : -1, -0.40 : -1, -0.50 : -1, -0.75 : -1, -1.00 : -1$ 双轴压试验. 单双轴压试块尺寸为 100 mm × 100 mm × 100 mm 立方体. 受压面的减摩垫层为 3 层塑料薄膜中间夹 3 层黄油. 测得了双轴主压方向的静态强度, 剖析了温度和应力比对单、双轴压强度发展趋势的影响规律以及试件破坏形态. 试验结果表明: 随温度的升高, 高温后高强高性能混凝土的单轴压强度并不一定降低; 双轴压强度相对于其单轴的提高倍数取决于应力比、不同温度等级后的高强高性能混凝土“脆硬性”. 提出了修正的带有温度和应力比参数高强高性能混凝土 Kupfer-Gerstle 破坏准则公式.

关键词: 高强高性能混凝土; 高温; 应力比; 单双轴压强度; 破坏准则

中图分类号: TU528.31; TU317⁺.3